Toxicology 384 (2017) 59–68

Contents lists available at ScienceDirect

Toxicology

journal homepage: www.elsevier.com/locate/toxicol

A paradoxical response of the rat organism to long-term inhalation of silica-containing submicron (predominantly nanoscale) particles of a collected industrial aerosol at realistic exposure levels

Marina P. Sutunkova[a], Svetlana N. Solovyeva[a], Boris A. Katsnelson[a,*], Vladimir B. Gurvich[a], Larisa I. Privalova[a], Ilzira A. Minigalieva[a], Tatyana V. Slyshkina[a], Irene E. Valamina[b], Oleg H. Makeyev[b], Vladimir Ya. Shur[c], Ilya V. Zubarev[c], Dmitry K. Kuznetsov[c], Ekaterina V. Shishkina[c]

[a] The Ekaterinburg Medical Research Center for Prophylaxis and Health Protection in Industrial Workers, Ekaterinburg, Russia
[b] The Central Research Laboratory of the Ural Medical University, Ekaterinburg, Russia
[c] School of Natural Sciences and Mathematics, the Ural Federal University, Ekaterinburg, Russia

ARTICLE INFO

Keywords:
Nano-silica containing industrial aerosol
Long-term inhalation exposure
Toxicity
Fibrogenicity
Toxicokinetics

ABSTRACT

While engineered SiO_2 nanoparticle toxicity is being widely investigated, mostly on cell lines or in acute animal experiments, the practical importance of as well as the theoretical interest in industrial condensation aerosols with a high SiO_2 particle content seems to be neglected. That is why, to the best of our knowledge, *long-term inhalation exposure* to nano-SiO_2 has not been undertaken in experimental nanotoxicology studies. To correct this data gap, female white rats were exposed for 3 or 6 months 5 times a week, 4 h a day to an aerosol containing predominantly submicron (nanoscale included) particles of amorphous silica at an exposure concentration of 2.6 ± 0.6 or 10.6 ± 2.1 mg/m^3. This material had been collected from the flue-gas ducts of electric ore smelting furnaces that were producing elemental silicon, subsequently sieved through a < 2 μm screen and redispersed to feed a computerized "nose only" inhalation system. In an auxiliary experiment using a single-shot intratracheal instillation of these particles, it was shown that they induced a pulmonary cell response comparable with that of a highly cytotoxic and fibrogenic quartz powder, namely DQ12. However, in long-term inhalation tests, the aerosol studied proved to be of very low systemic toxicity and negligible pulmonary fibrogenicity. This paradox may be explained by a low SiO_2 retention in the lungs and other organs due to the relatively high solubility of these nanoparticles. nasal penetration of nanoparticles into the brain as well as their genotoxic action were found in the same experiment, results that make one give a cautious overall assessment of this aerosol as an occupational or environmental hazard.

1. Introduction

In our previous experimental studies (Katsnelson et al., 2011, 2012a, 2012b, 2013, 2014, 2015; Privalova et al., 2014a, 2014b; Minigalieva et al., 2015, 2017), we have shown, in good agreement with the data of some other authors (e.g., Fröhlich, 2013; Fröhlich and Salar-Behzadi, 2014), that a single-shot intratracheal instillation and multiple intraperitoneal injections of a range of metal and metal-oxide nanoparticle (NP) species cause toxic effects "in vivo" at all levels, from cellular to systemic and organismic. These effects are considerably greater than the toxic effects of their micrometric chemical counterparts, one of the probable causes of this being the enhanced capability of such NPs to dissolve in biological media. On the other hand, the experiment with rats that were exposed to long-term inhalation of iron oxide (Fe_2O_3) NPs demonstrated that the overbalancing effect of the same solubility "in vivo" was low retention of these NPs in the organism and, thus, low pulmonary fibrogenicity and systemic toxicity (Sutunkova et al., 2016). It was of interest to test the hypothesis whether such paradoxically low harmfulness under inhalation exposure to cytotoxic nano-aerosols could be characteristic of other relatively easily solubilized NPs as well.

As we have repeatedly emphasized (e.g., Katsnelson et al., 2015), special interest in the toxicology of metal-oxide NPs is not due alone to the fact that they are purposefully manufactured (as so-called engi-

* Corresponding author.
E-mail address: bkaznelson@etel.ru (B.A. Katsnelson).

http://dx.doi.org/10.1016/j.tox.2017.04.010
Received 13 February 2017; Received in revised form 22 March 2017; Accepted 21 April 2017
Available online 24 April 2017
0300-483X/

neered nanoparticles) for various technological, scientific, and medical needs. Researchers in the field of nanotoxicology tend to underestimate the importance of the fact that people employed in metallurgical, welding and other industries and those residing in areas contaminated by atmospheric emissions from these facilities, find themselves being exposed chronically to such NPs that constitute a more or less substantial proportion of the submicron fraction of condensation aerosols by-produced in relevant “old” technologies. This renders the issue of metal and metal oxice nanotoxicology much more complex because these aerosols are, as a rule, both polydisperse and multi-component (Minigalieva et al., 2015, 2017).

The above is fully applicable to the condensation aerosols of such a typical *nonmetal* as silicon. These aerosols are released in the course of steel making (particularly when steel is being deoxidized with silicon in the ladle), production of ferrosilicon and other siliceous ferroalloys, arc welding (since all types of electrode coating include liquid glass, i.e. sodium silicate) and, above all, production of elemental silicon also called crystalline or metallic silicon.

This is an ore-thermal process conducted in an electric arc furnace with an open top through which crushed quartzite and coke are charged. The intermediate by-product of crystalline dioxide reduction to elemental silicon in this process is SiO monoxide. While in the furnace, this substance is in the gaseous state, being carried away from it with the outgoing stream of hot gases. But when it mixes with the ambient air being drawn in, it gets cooled and oxidized to silicon dioxide, SiO_2, which then condenses as a polydisperse aerosol consisting of spherical submicron-sized particles including a considerable percentage of nanoparticles (Velichkovsky and Katsnelson, 1964). It is this aerosol that furnace operators are exposed to at a concentration of 11,6 ± 2,2 mg/m^3 (Kulikov, 1995) and that is exhausted through the hood and downstream gas duct into the atmosphere. Similar concentrations of this aerosol at an average of 10,3 mg/m^3 were discovered by Petin (1975) in the workplace air near a furnace at a facility (producing ferrosilicon containing 75% of silicon.

As early as back in the late 1950s–early 1960s, B.T.Velichkovsky showed experimentally that SiO_2-containing condensation aerosols accompanying the production of various siliceous ferroalloys, can induce experimental silicosis, being sometimes even more fibrogenic than quartz dust (Velichkovsky and Katsnelson, 1964). These data were, however, obtained under intratracheal instillation of powders in standard doses (50 mg), i.e. under dust loads known to be excessive on rat lungs.

The only chronic inhalation experiment with such aerosols that lasted 6 months was, to the best of our knowledge, carried out by Petin (1978), who loaded into the dust feeders of 4 chambers operating in parallel dust samples swept off the plates of the electrodes on furnaces smelting ferrosilicon grades Si75, Si45 and Si18 (containing 82,9%, 61,0% and 30,8% of free silicon dioxide, respectively) or quartz dust (89,9% of free silicon dioxide in the form of alpha quartz). This researcher discovered, beyond any doubt, the onset of typical experimental silicosis which under exposure to aerosol with the highest concentration of amorphous silicon dioxide was even more intensive than under exposure to quartz dust. However, whereas two months after the termination of the inhalation exposure to quartz dust the silicotic pulmonary fibrosis continued progressing, the silicosis caused by the condensation aerosol with high SiO2 content demonstrated a reversal. The latter was explained by a much quicker clearance of the pulmonary tissue from SiO_2, which, in turn, could be explained by a greater solubility of the particles. In this case, too, we should emphasize the explicitly aggravated exposure conditions, with an average concentration of the aerosols in all chambers being 200 mg/m^3, i.e. 20 times higher than actual exposure levels.

A question arises whether it could be possible that for relatively low realistic levels of exposure the beneficial role of the solubility would prevail so much over its adverse effect that the ultimate changes in the lungs would prove to be very weak. This is exactly what was also observed by us (Sutunkova et al., 2016) in a chronic inhalation experiment with Fe_2O_3 nanoparticles at a low concentration (about 1 mg/m^3). However, although it is quite likely to be a general pattern, it needs verifying in each particular case.

In the above-mentioned experiment, Petin (1995) did not discover any dependence of the changes in some organs and systems of rats chronically inhaling condensation aerosols or quartz dust on silicon dioxide solubility, suggesting that the latter is as a favorable property which facilitates the elimination of silicon dioxide from the lungs without creating any danger of intoxication. However, this conclusion also needs to be verified both because in that experiment the researcher did not estimate the accumulation of silicon dioxide in various rat organs and blood and because the list of indices used for assessing the status of the organism was rather limited.

With the arrival of the «nanotechnology era», engineered nanoparticles of amorphous silica have become one of the five most widely consumed nano-products (Vance et al., 2015), and therefore compelled the attention of the toxicologists while understanding toxicological importance of inhalation exposures to spontaneously by-produced analogs of these NPs seems to have remained in the past. It is possibly why, given a great number of experiments with engineered SiO_2-NPs that have been carried out and are still conducted «in vitro» on cell cultures or, less often, «in vivo» in acute experiments under parenteral exposure (see, e.g., Park and Park, 2009; Eom and Choi, 2009; Kim et al., 2010; Sergent et al., 2012; Du et al., 2013; Petrick et al., 2016; Guo et al., 2015, 2016; Wang et al., 2017, and a lot of others), we have failed to find information on long-term inhalation exposure studies with this nanomaterial.

Recognising that such exposure is of real practical value in relation not so much to engineered SiO_2-NPs as to SiO_2-NPs component of the above-mentioned industrial aerosols, we set ourselves the task of conducting a chronic inhalation experiment to study the health effects of one of such aerosols in which, based on our earlier experience (Velichkovsky and Katsnelson, 1964), we could expect the presence of a substantial fraction of spontaneously by-produced SiO_2-NPs. Specifically, we have chosen for an inhalation study the submicron fraction of an aerosol emitted from silicon-producing ore-thermal furnaces.

The goal of this study was to not only characterize this particular aerosol but also come closer to verifying the general hypothesis stated previously: whether highly cytotoxic NPs can demonstrate low systemic toxicity and low pulmonary fibrogenicity on realistic inhalation exposure. As an independent test for particle cytotoxicity and acute pulmonotoxicity we used shifts in pulmonary free cell population in response to a single-shot intratracheal instillation of particles under study compared with those of DQ12 quartz. This test was long ago established as a good predictor of pulmonary fibrogenicity under long-term exposure to the micrometric particles (Katsnelson et al., 1994, 1995). However, we shall show that in the case of SiO_2-NPs this predictor can be deceptive due to toxicokinetic effects of these NPs solubilization.

2. Materials and methods

For a solid aerosol generator, we used the Palas RBG 1000 ID dispersing unit charged with a powder obtained by sieving through a < 2 μm screen the dust that had been collected in the horizontal section of the flue gas duct from the hood over an ore-thermal furnace. The scanning electron microscopy of this material revealed quantitative prevalence of particles of a regular spherical shape with a diameter of less than 100 nm (Fig. 1a).

It should be noted that the silicon smelting process in the ore-thermal furnace produces gaseous silicon monoxide, SiO, which gets oxidized and condenses to SiO_2 particles as the gas flow is cooled by the air being drawn along with it. There are no reasons to doubt that the above-mentioned spherical NPs and similar dia. > 100 nm submicron particles represent just the condensation aerosol of silicon dioxide.

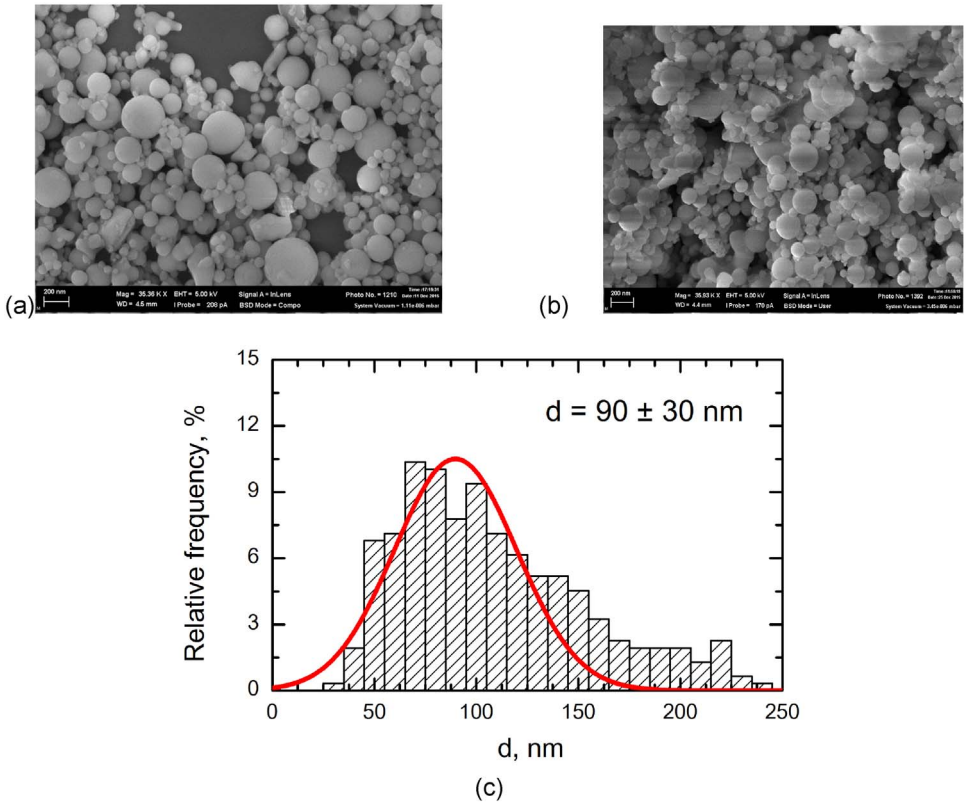

Fig. 1. (a) particles of the powder collected in the flue gas duct from the hood over a silicon smelting ore-thermal furnace and sieved through a < 2 μm screen; (b) a sample of suspended particles retained on a filter from the inhalation device with its particle feeder charged with this powder (scanning electron microscopy, magnification *35 930); (c) particle size distribution on the Image 1 (b).

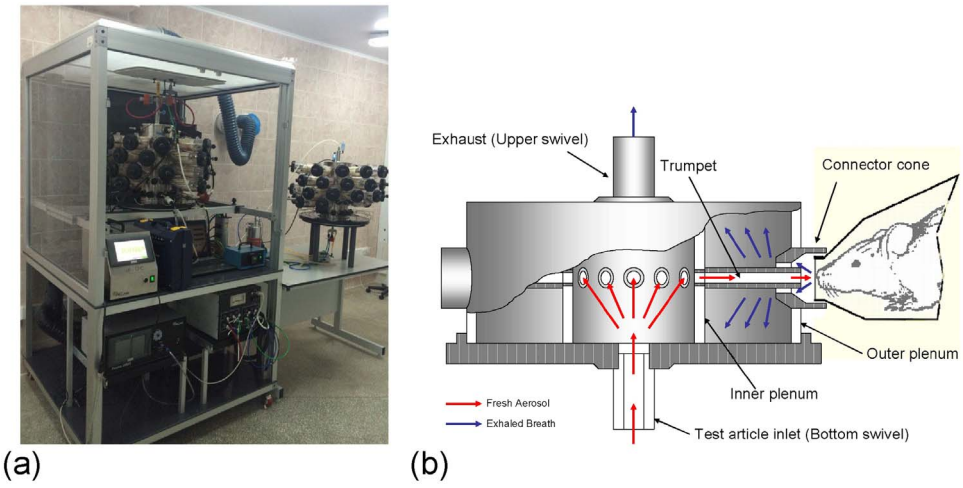

Fig. 2. (a) General view of the experimental setup (photographed with the front chamber doors removed). Next to the exposure unit, a similar system setup for sham exposure of control rats is shown. (b) Diagram of aerosol flows in the “nose only” inhalation exposure system (courtesy CH Technology, USA).

They are also prevalent in the SEM image (Fig. 1b and c) of the polycarbonate filter through which the air was drawn from the automatically controlled multi-tier “nose only” inhalation exposure system (CH Technologies, USA) for 60 rats (Fig. 2) at points corresponding to the breathing zone of the rats.

High-resolution visualization and measurement of the elemental composition of the nanoparticles on the filters were performed on a scanning electron microscope (SEM) AURIGA CrossBeam (Carl Zeiss NTS, Germany) equipped with an X-ray detector, X-Max (Oxford, UK). To enhance the image quality, the sample surface was coated with a sputtered thin carbon layer. The elemental composition was measured by energy-dispersive X-ray spectroscopy at an accelerating voltage of 5 kV. The spectra were collected in the centers of the nanoparticle clusters. This spectroscopy demonstrated that the NPs consisted predominantly of silicon and oxygen (see Fig. 3), the high spectral carbon peak corresponding mostly to the sputtered surface layer. Thus, the SEM analysis confirms our identification of the nanoparticles as SiO_2 condensation aerosol.

However, the SEM-images of both the source material and particles retained on the filters display also a small number of relatively large solitary particles of an irregular shape which are characteristic of disintegration aerosols, most likely carried off by the gas flow from the surface layers of the furnace top (quartzite and coke). This interpretation is confirmed by the chemical composition of the mixed aerosol, in

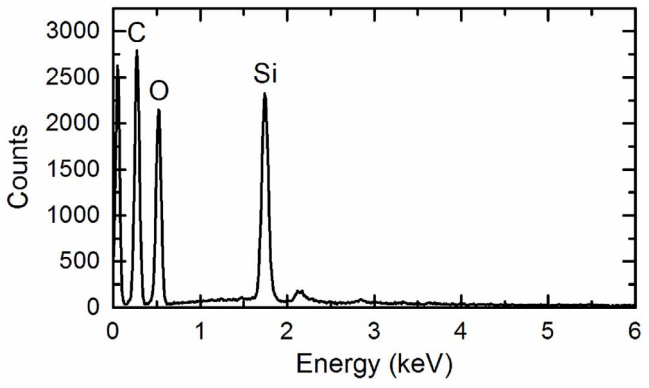

Fig. 3. Energy-dispersive X-ray spectrum collected in the center of a spherical nanoparticle cluster.

which we discovered 78% of free SiO_2, including 72% amorphous and only 6% crystalline. Hereinafter, this aerosol will be referred to as nano-silica containing aerosol (NSCA).

We operated the inhalation exposure system in two regimes, with an average concentration of 2.6 ± 0.6 mg/m^3 and 10.6 ± 2.1 mg/m^3. Under both regimes, the inhalation period (4 h a day, 5 times a week) lasted up to 6 months, with an intermediate term of 3 months when fractions of the test subjects were sacrificed.

Experiments were carried out on outbred white female rats (from our own breeding colony). All rats were housed in conventional conditions with natural light regime, breathed unfiltered air and were fed standard balanced food and clean bottled water. The study was planned and implemented in accordance with the "International guiding principles for biomedical research involving animals" developed by the Council for International Organizations of Medical Sciences (1985).

After the exposure period, the following procedures were performed for all rats:

- weighing;
- estimation of the CNS ability to induce temporal summation of subthreshold impulses – a variant of the withdrawal reflex and its facilitation by repeated electrical stimulations in an intact, conscious rat (Rylova, 1964);
- recording of the number of head-dips into the holes of a hole-board, which is frequently used for studying the behavioral effects of toxicants and drugs (e.g. Adeyemi et al., 2006; Fernandez et al., 2006);
- collection of daily urine for analysis of its density, urine output as well as biochemical indices presented by Table 2.

Then the rats were killed by decapitation and their blood was collected by exsanguination. The liver, spleen, kidneys, and brain were weighed. The biochemical indices determined from the blood are listed by Table 2 as well.

We used the MYTHIC-18 auto-hematology analyzer for determining the hemoglobin content, hematocrit, thrombocrit, mean erythrocyte volume and for counting RBC, WBC and thrombocytes. The proportion of reticulocytes was counted using the routine technique. Cytochemical determination of succinate dehydrogenase (SDH) activity in lymphocytes was based on the reduction of nitrotetrazolium violet to formazan, the number of granules of which in a cell was counted under immersion microscopy.

For DNA fragmentation testing, the samples of blood and femurs were promptly delivered in cryo-containers (−80 °C) to a specialized laboratory. To isolate DNA from the cells of blood and bone marrow, a GenElute (Sigma, St. Louis, MO,USA) set of reagents weas used. The DNA content of the samples was determined spectrophotometrically

Table 1
Number of cells in the bronchoalveolar lavage fluid (BALF) 24 h after intratracheal instillation of particle suspension to rats at a dose of 7 mg per 1 mL normal saline (x ± s.e.).

Substance administered	Number of cells * 10^6			NL/AM
	Total	Alveolar macrophages (AM)	Neutrophil leukocytes (NL)	
Nano-silica containing aerosol	5.85 ± 0.56*	3.03 ± 0.66	2.86 ± 0.79*	2.24 ± 1.16*
Quartz DQ_{12}	7.44 ± 1.30*	3.79 ± 0.94*	3.10 ± 0.80*	1.69 ± 0.64*
Normal saline (control group)	1.96 ± 0.29	1.49 ± 0.28	0.52 ± 0.24	0.37 ± 0.16

* Statistically significant difference from the control group ($P < 0.05$ by Student's *t*-test).

(Ultraspec 1100 pro; Amersham Biosciences Ltd.: Amersham, UK); then they were frozen and stored at −84 °C in a kelvinator (Sanyo Electric Co., Ltd.: Moriguchi, Japan) till the beginning of the RAPD (Random Amplified Polymorphic DNA) test performed as described by us earlier (Katsnelson et al., 2007). The method is based on the fact that, unlike a fragmented DNA, which, in the agarose gel electrophoresis, forms the so-called comet tail, a non-fragmented DNA has a very low degree of migration and virtually stays in the same place (comet head), the degree ofmigration being directly related to the degree of DNA fragmentation. DNA amplification was carried out using specific primers and tritiated nucleotides. To characterize the degree of damage to DNA we used the "coefficient of fragmentation", *i.e.*, the ratio of total radioactivity of all tail fractions to that of the head.

All the routine clinical laboratory tests on blood and urine were performed using well-known techniques described in many manuals (e.g. (Tietz, 1995).

We used as indices increase in which is characteristic of any experimental pneumoconioses: the dry mass of the lungs, total hydroxyproline content (in a colour reaction with *p*-dimethylaminobenzaldehyde), and total lipids (by the lung dry weight loss under extraction with ether in the Soxhlet extractor). Routine histological examination of the lung tissues and lung-associated lymph nodes was performed under optical microscopy of sections stained with hematoxylin-eosine or picrofuchsin (Van Gieson's staining), or impregnated with silver by Gomori's method. Besides, the pulmonary and brain accumulation of NPs was visualized by means of transmission electron microscopy (TEM). To this end, the pieces of an organ were fixed in 2% paraformaldehyde and 2.5% glutaraldehyde in a cacodylate buffer with 5% sucrose at pH 7.3, then post-fixed in 1% osmium tetroxide, contrasted with uranyl acetate en bloc and embedded in epoxy resin. This sample preparation procedure was carried out in a microwave tissue processor, HISTOS REM (Milestone, Italy). Semi-thin (900 nm thick) sections of epoxy blocks were stained in toluidine blue with the addition of 1% borax and examined under the optical microscope for choosing a site for TEM. The 60 nm ultrathin sections of this site obtained with the help a ultramicrotome (Power Tome, «RMC», USA) were treated for contrast with uranyl acetate and lead citrate. Grid-mounted sections were examined under an electron microscope, AURIGA («Carl Zeiss; MT», Germany) in the STEM mode in the range of magnifications 1200–2,00,000. The silicon contents of the lungs, liver, kidneys, spleen, blood and excreta was determined by atomic absorption analysis with electrothermal atomization on an atomic-absorption spectrophotometer ContrAA-700 (Analytik Jena AG) with preliminary preparation of samples by fusion of the biosubstrates in alkaline flux with subsequent dissolution.

Preliminarily, we carried out an experiment to study the cellular

Table 2
Indices for the organism of rats exposed inhalationally to Nano-silica containing aerosol (X ± s.e.).

Indices	Inhalation for 3 months			Inhalation for 6 months		
	Controls	NSCA 2.6 mg/m^3	NSCA 10.6 mg/m^3	Controls	NSCA 2.6 mg/m^3	NSCA 10.6 mg/m^3
Body mass before exposure, g	233.50 ± 2.62	240.11 ± 3.66	233.41 ± 2.39	229.20 ± 2.75	244.71 ± 2.73	240.36 ± 2.37
Body mass gain, %	18.12 ± 4.52	10.88 ± 0.84*	14.08 ± 1.26	16.86 ± 4.58	14.59 ± 1.77	19.79 ± 4.18
Temporal summation of sub-threshold impulses, sec	13.29 ± 0.43	11.71 ± 0.52*	13.37 ± 0.66	12.65 ± 0.41	10.99 ± 0.55	9.34 ± 0.52
Number of head-dips into holes during 3 min	5.11 ± 0.58	6.61 ± 0.74	6.80 ± 0.97	7.00 ± 0.81	4.00 ± 0.60	8.14 ± 0.67
Number of crossed squares during 3 min	8.16 ± 1.31	10.72 ± 1.73	14.00 ± 2.32*	17.32 ± 1.70	9.38 ± 1.86	19.14 ± 1.65
Liver mass, g per 100 g body mass	3.32 ± 0.08	3.24 ± 0.10	2.80 ± 0.42	3.00 ± 0.23	3.18 ± 0.06	3.32 ± 0.09
Kidney mass, g per 100 g body mass	0.60 ± 0.02	0.58 ± 0.01	0.51 ± 0.05	0.62 ± 0.03	0.62 ± 0.01	0.61 ± 0.01
Spleen mass, g per 100 g body mass	0.24 ± 0.01	0.22 ± 0.01	0.27 ± 0.05	0.22 ± 0.01	0.21 ± 0.01	0.23 ± 0.01
Brain mass, g per 100 g body mass	0.73 ± 0.02	0.70 ± 0.03	1.10 ± 0.44	0.76 ± 0.02	0.69 ± 0.02*	0.70 ± 0.01*
Hemoglobin, g/L	146.67 ± 2.00	154.22 ± 2.91*,•	144.22 ± 2.32	146.50 ± 2.97	153.64 ± 4.20	165.64 ± 15.84
Hematocrit, %	0.37 ± 0.01	0.40 ± 0.01*,•	0.37 ± 0.01	0.38 ± 0.01	0.39 ± 0.01	0.42 ± 0.04
Erythrocytes, 10^{12} cells/L	6.47 ± 0.10	6.84 ± 0.18	6.56 ± 0.12	6.68 ± 0.16	6.43 ± 0.35	7.41 ± 0.71
Leukocytes, 10^9/L	8.62 ± 0.42	10.27 ± 0.52*	11.51 ± 0.49*	10.20 ± 0.98	10.09 ± 0.66	12.78 ± 1.14
Thrombocytes, 10^9/L	781.78 ± 20.98	814.00 ± 25.22	809.56 ± 42.75	743.75 ± 30.28	755.45 ± 45.88	668.55 ± 38.78
Lymphocytes,%	72.00 ± 1.41	72.11 ± 1.12	70.33 ± 1.13	73.00 ± 1.04	73.73 ± 0.93*	69.82 ± 1.55
Banded neutrophils, %	0.89 ± 0.11	1.56 ± 0.24*	1.44 ± 0.24*	1.50 ± 0.19	1.00 ± 0.00*	1.27 ± 0.14
Segmented neutrophils, %	20.11 ± 1.10	19.67 ± 0.83	21.22 ± 0.91	17.00 ± 0.94	16.27 ± 0.81•	20.64 ± 1.37*
Monocytes,%	5.00 ± 0.47	4.22 ± 0.40	4.44 ± 0.50	5.63 ± 0.65	6.82 ± 0.50	5.64 ± 0.39
Eosinophils,%	2.00 ± 0.24	2.44 ± 0.44	2.56 ± 0.53	2.88 ± 0.52	2.18 ± 0.46	2.64 ± 0.43
Basophils, %	0 ± 0	0 ± 0	0 ± 0	0 ± 0	0 ± 0	0 ± 0
Succinate dehydrogenase (SDH) activity, number of formazane granules per 50 lymphocytes	578.89 ± 36.51	537.78 ± 19.20	581.33 ± 13.78	674.00 ± 25.04	707.17 ± 12.12	722.00 ± 26.88
Bilirubin in blood serum, μmol/L	1.88 ± 0.24	2.31 ± 0.40	2.51 ± 0.32	2.31 ± 0.17	2.39 ± 0.22	2.04 ± 0.18
Total protein content of blood serum, g/L	81.32 ± 1.31	80.11 ± 1.15	80.83 ± 1.10	80.71 ± 3.07	80.25 ± 1.86	81.48 ± 1.63
Albumin content of blood serum, g/L	52.49 ± 1.48	49.79 ± 1.03	49.23 ± 0.81	45.44 ± 1.93	47.11 ± 1.36	46.36 ± 1.34
Globulin content of blood serum, g/L	30.32 ± 0.95	31.60 ± 1.30	28.83 ± 0.61	33.14 ± 1.35	35.12 ± 1.28	35.27 ± 1.91
A/G index	1.83 ± 0.08	1.66 ± 0.07	1.59 ± 0.09*	1.31 ± 0.08	1.45 ± 0.07	1.34 ± 0.07
AST activity in blood serum, mM/h L	226.22 ± 21.88	253.32 ± 24.34	283.62 ± 36.59	413.61 ± 51.17	294.58 ± 17.58*	297.77 ± 32.25
ALT activity in blood serum, mM/h L	53.10 ± 4.09	55.52 ± 4.05	56.03 ± 4.94	120.95 ± 30.01	75.35 ± 6.20	74.62 ± 11.31
De Ritis coefficient	4.27 ± 0.30	4.54 ± 0.28	5.05 ± 0.40	4.06 ± 0.46	4.02 ± 0.22	4.15 ± 0.19
SH-groups in blood plasma, mmol/L	0.44 ± 0.03	0.43 ± 0.07	0.42 ± 0.05	0.53 ± 0.23	0.76 ± 0.17	0.67 ± 0.28
Uric acid in blood serum, μmol/L	86.33 ± 9.70	95.89 ± 9.29	90.11 ± 10.52	154.88 ± 14.49	124.55 ± 7.42	124.09 ± 11.48
Urea in blood serum, mmol/L	4.71 ± 0.32	4.58 ± 0.23	4.28 ± 0.26	5.28 ± 0.45	4.42 ± 0.24	4.84 ± 0.45
Alkaline phosphatase in blood serum, IU/L	101.90 ± 10.94	70.57 ± 9.27*	64.20 ± 3.17*	86.93 ± 13.66	74.68 ± 4.59	99.23 ± 15.80
Catalase in blood serum, μmol/L	0.90 ± 0.12	0.92 ± 0.10	0.87 ± 0.09	1.33 ± 0.05	1.40 ± 0.03	1.34 ± 0.04
Reduced glutathione in whole blood, μmol/L	20.99 ± 5.75	23.44 ± 5.65	25.87 ± 7.88	22.05 ± 1.66	18.52 ± 1.17	18.16 ± 1.29
Ceruloplasmin in blood serum, mg/%	146.39 ± 14.09	157.08 ± 10.68•	195.56 ± 6.27*	109.22 ± 7.30	111.78 ± 9.85	146.31 ± 14.63*
MDA in blood serum, μmol/L	3.60 ± 0.18	3.65 ± 0.16	3.75 ± 0.29	6.47 ± 0.33	5.59 ± 0.20*	4.98 ± 0.31*
Glucose in blood serum, mmol/L	6.67 ± 0.18	6.81 ± 0.21	6.73 ± 0.34	7.61 ± 0.21	7.74 ± 0.30	7.08 ± 0.34
Amilase in blood serum, IU/L	3416.00 ± 448.36	3245.67 ± 217.09	2917.11 ± 61.01	4306.63 ± 650.33	3799.64 ± 191.25	3964.73 ± 395.29
γ-glutamyltransfe-rase in blood serum, IU/L	2.22 ± 0.94	3.41 ± 0.63	3.83 ± 1.20	6.40 ± 2.40	4.16 ± 0.68	9.24 ± 3.69
Diuresis, mL	50.11 ± 3.56	53.17 ± 2.25•	42.24 ± 4.50	45.21 ± 2.53	42.00 ± 2.90	42.33 ± 3.14
Total protein in urine, mg/L	146.31 ± 13.82	115.49 ± 9.22	125.83 ± 7.14	97.50 ± 8.20	92.42 ± 12.16	91.42 ± 17.88
Urea in urine, mmol/L	71.25 ± 2.56	66.58 ± 1.74	88.08 ± 10.54	87.36 ± 3.49	91.25 ± 3.83	84.56 ± 4.62
Uric acid in urine, μmol/L				65.00 ± 5.40	73.05 ± 6.05	58.33 ± 6.77
Creatinine in urine, mmol/L	0.84 ± 0.06	0.78 ± 0.03	0.85 ± 0.05	0.87 ± 0.03	0.97 ± 0.04	0.87 ± 0.04
Coproporphyrin in urine, nmol/L	38.87 ± 6.75	69.05 ± 8.97*	45.40 ± 8.21	50.57 ± 9.42	37.16 ± 8.25	37.28 ± 7.77
Bilirubin in urine, μmol/L				1.56 ± 0.13	1.73 ± 0.11	1.72 ± 0.19

* Denotes the quantities that are statistically significantly different from corresponding controls ones ($p < 0.05$ by Student's *t*-test with Bonferroni correction).
• Denotes statistically significant difference between two experimental groups ($p < 0.05$ by Student's *t*-test with Bonferroni correction).

response of the lower airways in rats exposed to a single-shot intratracheal instillation of the nano-silica containing aerosol 24 h before bronchoalveolar lavage. This was done in comparison with a response to standard quartz dust DQ_{12}, a material having particle sizes of less than 5 μm and free SiO_2 content of ca. 80% (Robock, 1973). To carry out bronchoalveolar lavage, a cannula connected to a Luer's syringe containing 10 mL of normal saline was inserted into the surgically prepared trachea of a rat under hexenal anesthesia. The fluid entered the lungs slowly under the gravity of the piston, with the animal and syringe positioned vertically. Then the rat and the syringe were turned 180°, and the bronchoalveolar lavage fluid (BALF) flowed back into the syringe. The extracted lavage fluid was transferred to siliconized refrigerated tubes. An aliquot sample of the lavage fluid was drawn into a WBC count pipette together with 3% acetic acid and

Table 3
Some indices for the status of rat lungs after inhalation exposure to particles of Nano-silica containing aerosol (X ± s.e.).

Indices	Inhalation, 3 months			Inhalation, 6 months		
	Controls	SiO_2 2.6 mg/m^3	SiO_2 10.6 mg/m^3	Controls	SiO_2 2.6 mg/m^3	SiO_2 10.6 mg/m^3
Lung mass, g per 100 g body mass	0.75 ± 0.04	0.89 ± 0.05*	1.08 ± 0.07*,•	1.05 ± 0.15	0.89 ± 0.07	0.97 ± 0.10
Dry lung mass, g per 100 g body mass	0.08 ± 0.01	0.08 ± 0.01	0.09 ± 0.01•	0.17 ± 0.02	0.17 ± 0.02	0.16 ± 0.01
Absolute lipid content of lungs, mg	33.82 ± 2.74	31.84 ± 2.98	37.66 ± 4.57	68.02 ± 5.63	36.98 ± 4.81*	60.64 ± 4.56
Absolute hydroxyproline content of lungs, μg	2060.53 ± 84.60	4977.58 ± 1187.24*	4641.25 ± 1022.41*	4112.15 ± 578.34	3048.12 ± 532.91	6141.72 ± 945.94•
Hydroxyproline content of lungs, μg per 100 g body mass	775.92 ± 40.75	1897.81 ± 458.68*	1711.90 ± 380.78*	1652.98 ± 208.81	1145.94 ± 209.42	2227.05 ± 342.47•

* Denotes values which are statistically significantly different from corresponding control values ($p < 0.05$ by Student's *t*-test).
• Denotes a statistically significantly difference between two experimental grops of one and the same exposure period ($p < 0.05$ by Student's *t*-test).

methylene blue. Cell count was performed in a standard hemocytometer (the so-called Goryayev's chamber). For cytological examination, the BALF was centrifuged for 4 min at 200*g*, then the fluid was decanted and the sediment was used for preparing smears on two microscope slides. After air drying, the smears were fixed with methyl alcohol and stained with azure eosin. The smears were examined microscopically with immersion at ×1000 magnification. The differential count for determining the percentage of AMs, NLs, and other cells was conducted up to a total number of 100 counted cells. Allowing for the number of cells in the BALF, these percentages were recalculated in terms of absolute AM and NL counts.

To characterize NSCA particles solubilization, a batch of the powder was incubated at 37 °C together with either the normal saline, or the Ringer-Locke's solution, or the cell-free BALF supernatant in ratio 2 mg per 10 mL. Samples of each system were taken at time points 1, 3, 5, 7, 9 and 24 h, centrifuged and analyzed for the Si content with the help of AAS (atomic absorption spectrometry).

3. Results

The 3-4-fold increase in the total cell count of the BALF after intratracheal instillation of particles due to enhanced recruitment of alveolar macrophages (AM) and, especially, neutrophil leukocytes (NL) into the lower airways (see Table 1) is a well-studied compensatory response to the impact of products of macrophage breakdown caused by phagocytized dust particles (Privalova et al., 1980; Katsnelson et al., 1995), including nanoscale ones (e.g., Privalova et al., 2014b; Katsnelson et al., 2014). Judging from these indices, the cytotoxicity of Nano-silica containing aerosol (NSCA) and quartz DQ12 is quite similar.

In the long-term inhalation experiment, the general condition of the rat organism was assessed against a great number of indices listed in Table 2.

Although some values in the two groups show a statistically significant departure from the control value for this or that concentration over this or that exposure period, the fact that these departures do not demonstrate dose or time dependence on exposure conditions does not allow us to identify them with confidence as NSCA effects. At the same time, although some departures are not sufficiently statistically significant, they tend to be dependent on the level of exposure. In particular, decrease in the threshold impulse summation index measured in a variant of the withdrawal reflex and its facilitation by repeated electrical stimulations in an intact, conscious rat (Rylova, 1964), which may testify to prevalence of CNS excitation over inhibition, was more pronounced towards the end of the 6-month exposure period at the concentration of 10.6 mg/m^3 than at the concentration of 2.6 mg/m^3. However, this type of dependence on exposure level was not found in 3-month inhalation exposure, nor for other indices of the central nervous system functioning (number of head dips and number of squares crossed in 3 min). In general, the obvious conclusion is that the Nano-silica containing aerosol did not display systemic toxicity even at a relatively high concentration and longer exposure period.

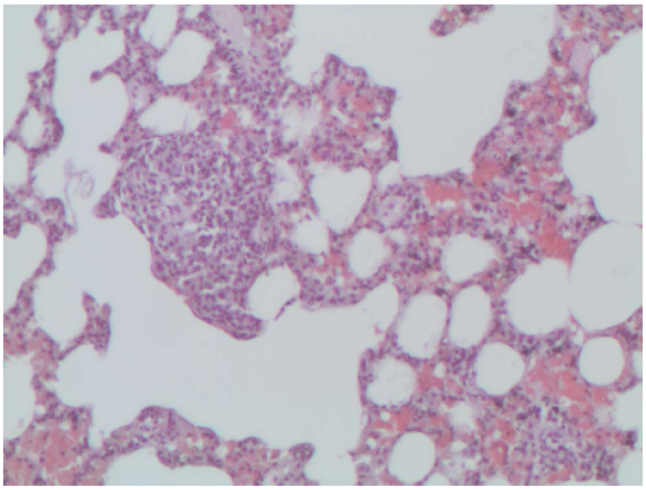

Fig. 4. Rat lungs after inhalation exposure to Nano-silica containing aerosol at the concentration of 10.6 mg/m^3 during 6 months. Alveolar septa are thickened, with lymphocytic infiltration, but round macrophage-lymphocytic clusters occur as solitary observations only. Hematoxylin and eosin staining, magnification X 50.

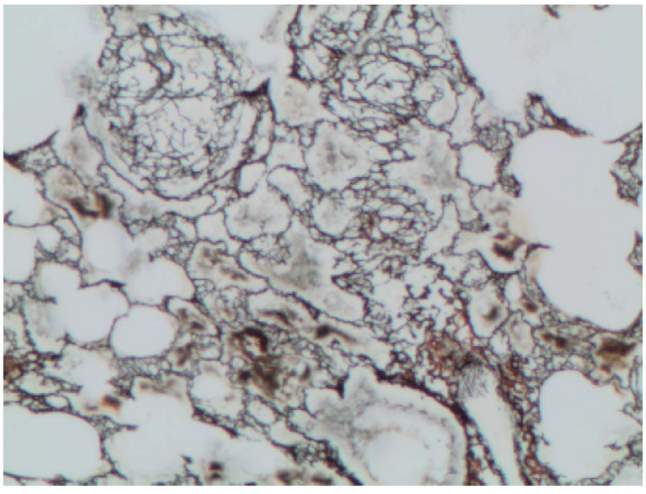

Fig. 5. Rat lungs after inhalation exposure to Nano-silica containing aerosol at the concentration of 10.6 mg/m^3 during 6 months. Focal coarsening of the argyrophylic structure in the lung tissue and appearance of a net of thin argyrophylic fibers within a macrophagal-lymphocytic nodule. Gomori's silver stain. Magnification X 100.

However, the main target organ for inhaled free silica particles (both crystalline, and amorphous) are the lungs, in which these

Table 4
Silicon SiO_2 content of the rat organs, blood and excreta (x ± s.e.).

Exposureperiod,mnths	Group	Organs,mg						Blood,mg/L	Urine,mg/L	Feces, mg/g
		lungs	lungs-associa-tedlymphnodes [1]	liver	kidneys	spleen	brain			
theexposureconcentrationofNSCA2.6mg/m^3										
3	EXPOSED	0.114 ± 0.022*	0.014	0.022 ± 0.003*	0.025 ± 0.003*	0.024 ± 0.004	0.016 ± 0.002	0.39 ± 0.16*	1.47 ± 0.21*	2.18 ± 0.12*
	CONTROL	0.023 ± 0.005	0.004	0.012 ± 0.006	0.012 ± 0.006	0.021 ± 0.005	0.013 ± 0.002	0.24 ± 0.06	0.44 ± 0.07	1.36 ± 0.10
6	EXPOSED	0.202 ± 0.013*,+	0.055	0.041 ± 0.006*,+	0.044 ± 0.006*,+	0.047 ± 0.006*,+	0.018 ± 0.002	0.46 ± 0.04*,+	1.68 ± 0.07*,+	2.32 ± 0.28*
	CONTROL	0.036 ± 0.006	0.005	0.014 ± 0.002	0.013 ± 0.001	0.018 ± 0.003	0.014 ± 0.001	0.27 ± 0.04	0.44 ± 0.07	1.38 ± 0.08
the exposure concentration of NSCA 10,6 mg/m^3										
3	EXPOSED	0.630 ± 0.067*,@	0.024	0.033 ± 0.004*,@	0.036 ± 0.007*,@	0.062 ± 0.007*,@	0.016 ± 0.002	0.60 ± 0.14*,@	4.57 ± 0.23*,@	7.24 ± 0.30*,@
	CONTROL	0.023 ± 0.005	0.004	0.012 ± 0.006	0.012 ± 0.006	0.021 ± 0.005	0.013 ± 0.002	0.24 ± 0.06	0.44 ± 0.07	1.36 ± 0.10
6	EXPOSED	0.742 ± 0.052*,+,@	0.063	0.061 ± 0.007*,+,@	0.070 ± 0.006*,+,@	0.072 ± 0.002*,+,@	0.018 ± 0.001	0.71 ± 0.05*,+,@	3.06 ± 0.11*,+,@	4.39 ± 0.53*,+,@
	CONTROL	0.036 ± 0.006	0.005	0.014 ± 0.002	0.013 ± 0.001	0.018 ± 0.003	0.014 ± 0.001	0.27 ± 0.04	0.44 ± 0.07	1.38 ± 0.08

[1] Determined in the each group of rats' pooled tissue and divided by the number of rats in the group.
* Denotes values which are statistically significantly different from the control value for the same exposure period ($p < 0.05$ by Student's *t*-test).
+ Denotes values which are statistically significantly different from the index obtained for the same exposure period at the lower concentration ($p < 0.05$ by Student's *t*-test).
@ Denotes values which are statistically significantly different from the value obtained for the previous exposure period at the same concentration.

Table 5
Kinetics of NSCA particle dissolution in various milieus (incubation at 37 °C at a ratio of 1 mg NSCA per 10 mL of milieu).

Duration of incubation, hours	Concentration of silicon in solution, mg/L		
	BALF supernatant	Normal saline	Ringer-Locke's solution
1	7.10	1.41	3.35
3	11.95	3.33	4.7
5	12.39	4.45	5.54
7	14.10	5.54	6.12
9	15.67	6.12	7.74
24	18.20	8.25	6.76

particles are commonly capable of causing the nodular fibro productive process known to be the experimental model of silicosis, one of the most serious occupational diseases (Velichkovsky and Katsnelson, 1963; Katsnelson et al., 1995; Honnons and Porcher, 2000 and many others). One of its common manifestations is an increase in the relative mass of the lungs. However, as follows from Table 3, being statistically significantly and dose-dependently increased in the 3-month period, this index was found to be even lower than the control value in the 6-month period.

Moreover, the relative dry mass of the organ was not increased for either of the aerosol concentrations in any of the exposure periods. Neither did we observe any increase in such a sensitive index of the pneumoconiotic process as absolute lipid content of the lungs (Katsnelson et al., 1995), while enhanced collagen biosynthesis, which is typically characteristic of silicosis manifesting itself in increased total hydroxyproline content of the lungs, was statistically significant for 3 months only, being, however, practically independent of exposure level.

This insignificant response of the above-considered experimental silicosis indices differs from the literature data on the effect of micrometric and submicron particles of silica, specifically, of quartz, and from the long experience of our laboratory in this area. This experience was gained, however, in experiments with much higher concentrations of quartz dust (e.g., Katsnelson et al., 1984, 1987, 1994) or even amorphous silica gel disintegration aerosol (Katsnelson et al., 1984). At the same time, in the present experiment such a low level of response is in full agreement with the results of morphological examination of pulmonary tissue preparations.

At the concentration of 10.6 mg/m^3 only, the enlarged alveolar septa showed solitary clusters of dust particles and round cellular nodules towards the end of the 6-month exposure period (Fig. 4). However, there are no collagen fibers around or within the nodules, although Gomori silver staining revealed a net of thin argyrophilic reticular fibers (Fig. 5), which point to an early stage of nodular sclerosis. The tracheobronchial lymph nodes reveal cellular nodules also with very early signs of sclerosis.

As can be seen from Table 4, the chemically determined silica content of the lungs and lungs-associated lymph nodes is substantially higher than in the controls, this increase being dependent on both the level and the duration of the inhalation exposure, which confirms its causal relationship with the latter.

However, according to Bellmann et al. (1991), approximately the same extent of retention of SiO_2 in rat lungs (0.550 mg) was observed over 6 months under a similar inhalation exposure to standard quartz dust DQ12 at a concentration of 1 mg/m^3, which is 10 times lower than in our experiment with Nano-silica containing aerosol. In other words, if calculated per unit concentration of aerosol in the air, the accumulation of SiO_2-NPs in the lungs under chronic inhalation exposure to NSCA is approximately 10 times less than the accumulation of SiO_2 under similar inhalation exposure to quartz dust DQ12.

Since equal doses of DQ12 and NSCA particles produce a roughly

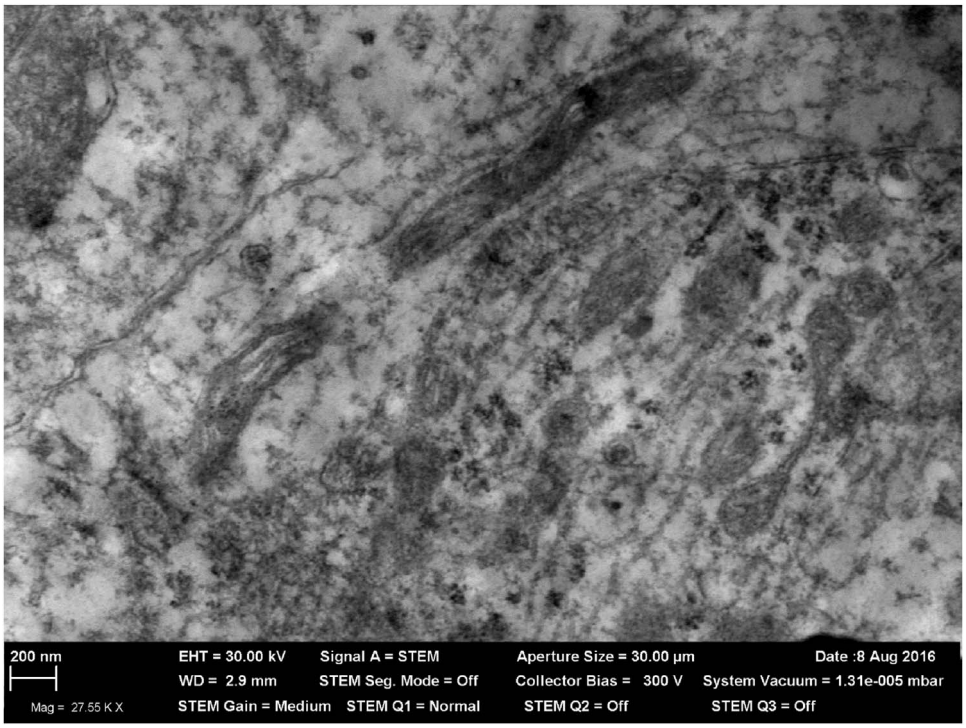

Fig. 6. Nanoparticles in the neuron body under inhalation exposure to Nano-silica containing aerosol at the concentration of 2.6 mg/m^3 during 3 months. STEM, magnification X 27550.

similar effect on the pulmonary phagocytic self-clearance mechanism (Table 1), the substantial difference in their retention in the lungs can only be explained by presuming that in the case of Nano-silica containing aerosol, the most important role belongs not to this physiological mechanism but to physicochemical clearance associated with the dissolution of submicron (nanoscale, in particular) silica particles «in vivo», especially in the lining fluid of the pulmonary area on which they deposit when inhaled. This mechanism is modeled «in vitro» by a noticeable dissolution of particles in the BALF supernatant of intact rats (Table 5). The dissolution of SiO_2 particles from NSCA in the Ringer-Locke's solution imitating the ionic composition of body fluids is less active but still more active than in the normal saline.

At the same time, transmission electron microscopy confirms that NSCA particles are retained in the lungs, though in a small amount. However, in spite of their high cytotoxicity, this amount of nanoparticles did not cause any essential pathological changes in the pulmonary tissue.

The dissolution of SiO_2 undoubtedly leads to a dose-dependent increase in the concentration of silicon in the blood and, consequently, in the urine, as well as in internal organs. An appreciable increase in the feces SIO_2 concentration may also be partly linked to its transition from the blood into the liver (in which it is really elevated – see Table 4) and thence to the intestines with the bile. On the other hand, it may be explained by the physiological mechanism of airways self-clearance along the pathway 'trachea–pharynx–esophagus'. However, we find it difficult to explain why both the urine and the feces of rats exposed to the higher NSCA level had significantly lower concentrations of silicon in the second exposure period compared with the first one.

The resorption of the substance from an organ of primary particle retention into the blood stream resulting in not only its accelerated elimination from the organism but also in its accumulation in various organs is a prerequisite to systemic toxicity. In our case, however, no marked manifestations of it were found. In other words, actual accumulation of silicon in organs (determined by the dynamic equilibrium between particle entry from the blood into organs and reverse elimination from organs into the blood, one of the causes of which is the same dissolution of NSCA particles in the tissues) was below the threshold of its toxic effects.

Table 6
Genomic DNA fragmentation coefficient for blood and bone marrow cells of rats exposed to Nano-silica containing aerosol particles during 6 months (RAPD-test) (x ± s.e.).

Tissue	Controls	SiO_2 concentration	
		2.6 mg/m^3	10.6 mg/m^3
Nucleated blood cells	0.4240 ± 0.0005	0.4622 ± 0.0004*	0.4704 ± 0.0005*,•
Bone marrow	0.3995 ± 0.0005	0.4043 ± 0.0003*	0.4316 ± 0.0003*,•

* Denotes values which are statistically significantly different from corresponding control ones ($p < 0.05$ by Student's *t*-test).
• Denotes a statistically significant difference between two experimental groups ($p < 0.05$ by Student's *t*-test).

The ability of inhaled nanoparticles initially deposited in the nasal passages to penetrate along the olfactory nerve fibers into the olfactory area of the brain known from the literature (Oberdörster et al., 2004; Elder et al., 2006; Kao et al., 2012) has been confirmed in our experiment as well. As follows from Fig. 6, even the rats that were exposed to the lower concentration of the aerosol reveal a considerable number of nanoscale electron-dense round formations in some neurons of this area.

These formations are most likely to be nanoparticles of the aerosol under study. As for the results of chemical determination of SiO_2 content of the whole brain, however, only a very small increase in it was observed for both exposure periods (Table 4). We observed no clear signs of disturbance to the ultrastructure of the particle-loaded neuron. As noted above, neither did we find any reliable deviations in the rat brain activity indices. It should be noted, however, that the relative brain mass towards the end of the 6-month exposure period was for both exposure levels statistically significantly lower than the respective control value. Although rarely observed, this effect is nevertheless known to be associated with the impact of some neurotoxic substances, for example, the synthetic pyrethroid cypermethrin (Grewal et al., 2010).

As can been seen from Table 6, the enhanced fragmentation of the

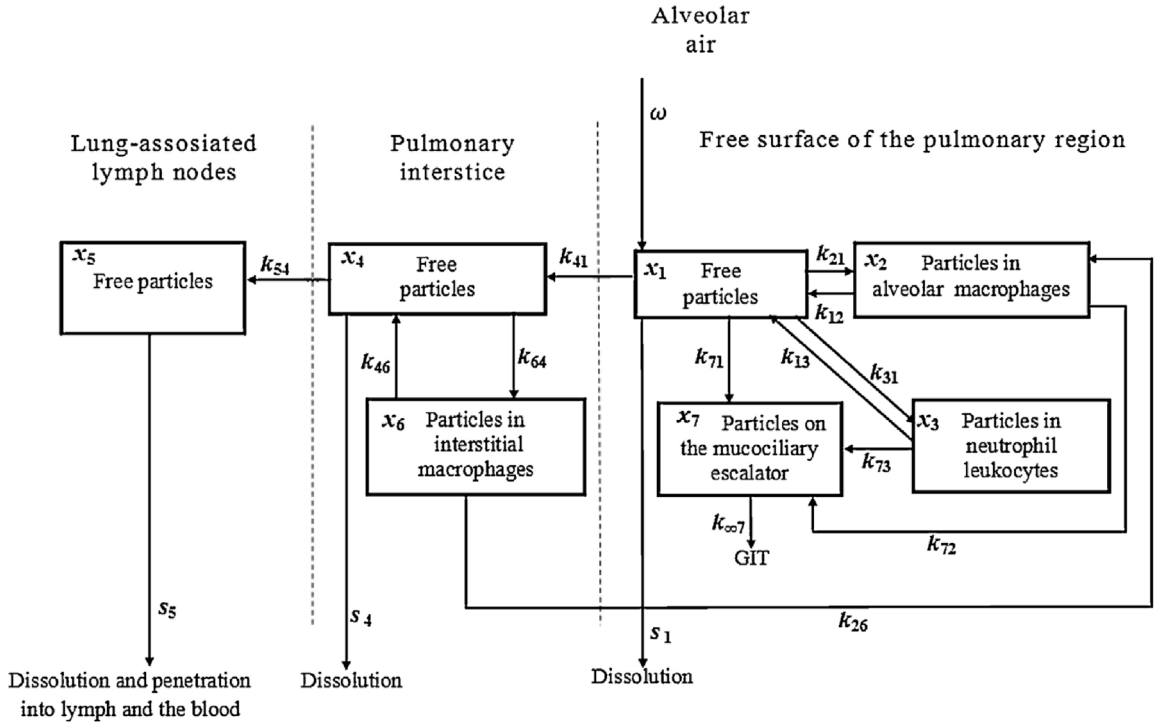

Fig. 7. Structure of the multi-compartmental model for the kinetics of retention and elimination of NPs deposited in the pulmonary region of the lung (reproduced from Sutunkova et al., 2016). Here: ω is a function of particle deposition in the pulmonary region, and k_{ji} is a rate constant of particle translocation from compartment X_i into compartment X_j. Dotted lines are conventional boundaries between anatomical regions.

genomic DNA was found in both nucleated blood cells and bone marrow cells, the latter clearly displaying the dependence of this effect on the exposure level.

4. Discussion

First of all, it should be stressed that even the highest of 2 exposure levels tested in our inhalation experiment (ca. 10 mg/m^3) can be considered realistic, taking into consideration that it corresponds to average concentrations of amorphous SiO_2 containing aerosols to which workers are exposed in elemental silicon and in ferrosilicon productions (see Introduction). On the other hand, it is much higher compared with the maximal acceptable concentration (MAC) officially established in Russia for industrial aerosols containing > 60% amorphous SiO_2 (namely, 1 mg/m^3). Assuming that this MAC is safe by definition, it was important to assess possible adverse effects of long-term experimental exposure to the concentration 2–3 times higher. The factual average concentration of 10.6 ± 2.1 mg/m^3 and 2.6 ± 0.6 mg/m^3, respectively, proved *post factum* to have been in good accordance with the desired ones.

The cellular response of the lower airways to the deposition of submicron (mainly nanoscale) particles containing amorphous silicon dioxide as the main chemical component points to their high cytotoxicity. Despite this, their ability to cause silicosis in lungs under chronic inhalation exposure even at a level which is 10 times the maximum allowable concentration in workroom air established for such an aerosol in Russia was found to be rather low. The nearest cause of this paradoxical mismatch between these two harmful effects, which are typically closely linked under the impact of silica-containing aerosols (Katsnelson et al., 1984, 1995), is the low accumulation of silicon dioxide in lungs, which can be explained by the relatively high solubility of these particles within the lung.

Most likely, in this case, as well as in the case of iron oxide nanoparticles which we studied earlier (Sutunkova et al., 2016), this dissolution plays the role of an essential additional mechanism of pulmonary particle clearance along with the penetration of particles into the lymph and/or directly into the blood, and their mucociliary activity-driven translocation into the digestive tract. We believe it possible to preliminarily describe these processes by the same multi-compartmental model that was developed and quantitatively identified by us for Fe_2O_3-NPs (Fig. 7) although its conclusive generalization to a certain class of nanoparticles will require new experiments (with metal NPs characterized by relatively low solubility).

Solubility is also a precondition to the diffusion of the resulting silicic acid in the blood and, thus, to the enhanced resorptive toxicity of NSCA but, at the same time, an important factor reducing the accumulation of SiO_2 in tissues, which for the given exposure levels proved to be insufficient to cause clear signs of chronic intoxication.

Nevertheless, caution should be exercised in an expert assessment of the aerosol under study considering, first, the ability of NSCA particles to penetrate the brain. Although transnasal penetration of any inhaled NPs into the brain seems to be inevitable and although we have not found any reliable data demonstrating the damaging impact of these NPs on the brain either in the literature or in our experiment, we believe that the potential risk of such impact should be taken into consideration in the overall safety and toxicity evaluation of the aerosol under study.

Besides, such cautious assessment cannot but take into consideration the genotoxic «in vivo» effect of this aerosol. In fact, this genotoxicity proved to be the only undoubtedly dose-dependent effect of the aerosol under consideration for the realistic exposure levels tested. Note that the multi-organ genotoxicity «in vivo» under subchronic intoxications caused by repeated intraperitoneal injections is characteristic of practically all metal and metal-oxide nanoparticles studied by us so far (Katsnelson et al., 2015). In the present study using even more adequate experimental model we have revealed the systemic genotoxicity of the NSCA not only as an especially dangerous but also as the most sensitive effect of chronic nano-toxicity.

5. Conclusions

The silica (mostly amorphous) containing submicron particles with a prevailing proportion of those in the nanoscale range induce, when instilled intratracheally, a pulmonary cell response comparable with that to highly cytotoxic and fibrogenic standard quartz powder DQ12. Nevertheless, in long-term inhalation experiments at realistic concentrations, they proved to be of very low systemic toxicity and negligible pulmonary fibrogenicity. This paradox may be explained by low SiO_2 retention in lungs and other organs due to a relatively high solubility of these nanoparticles in relevant biological and model milieus. However, their genotoxic action and transnasal penetration into the brain found in the same inhalation experiment should make one give a cautious overall assessment of this aerosol as an occupational or environmental hazard.

References

Adeyemi, O.O., Yemitan, O.K., Taiwo, A.E., 2006. Neurosedative and muscle-relaxant activities of ethyl acetate extract of Baphianitida AFZEL. J. Ethnopharmacol. 106, 312–316.

Bellmann, B., Creutzenberg, O., Dasenbrock, C., 1991. Lung clearance and retention of toner utilizing a tracer technique: during chronic inhalation exposure in rats. Fundam. Appl. Toxicol. 17, 300–313.

Du, Z.J., Zhao, D.L., Jing, L., Cui, G., Jin, M., Li, Y., Liu, X., Liu, Y., Du, H., Guo, C., Zhou, X., Sun, Z., 2013. Cardiovascular toxicity of different sizes amorphous silica nanoparticles in rats after intratracheal instillation. Cardiovasc. Toxicol. 13 (3), 194–207.

Elder, A., Gelein, R., Silva, V., Feikert, T., Opanashuk, L., Carter, J., Potter, R., Maynard, A., Ito, Y., Finkelstein, J., Oberdörster, G., 2006. Translocation of inhaled ultrafine manganese oxide particles to the central nervous system. Environ. Health Perspect. 114 (8), 1172–1178.

Eom, H.J., Choi, J., 2009. Oxidative stress of silica nanoparticles in human bronchial epithelial cell, Beas-2B. Toxicol. In Vitro 23 (7), 1326–1332.

Fernandez, S.P., Wasowski, C., Loscalzo, L.M., Granger, R.E., Johnston, G.A., Paladini, A.C., Marder, M., 2006. Central nervous system depressant action of flavonoid glycoside. Eur. J. Pharmacol. 539, 168–176.

Fröhlich, E., Salar-Behzadi, S., 2014. Toxicological assessment of inhaled nanoparticles: role of in vivo, ex vivo, in vitro, and in silico studies. Int. J. Mol. Sci. 15, 4795–4822.

Fröhlich, E., 2013. Cellular targets and mechanisms in the cytotoxic action of non-biodegradable engineered nanoparticles. Curr. Drug Metab. 14 (9), 976–988.

Grewal, K.K., Sandhu, G.S., Kaur, R., Brar, R.S., Sandhu, H.S., 2010. Toxic impacts of cypermethrin on behavior and histology of certain tissues of albino rats. Toxicol. Int. 17 (2), 94–98.

Guo, C., Xia, Y., Niu, P., Jiang, L., Duan, J., Yu, Y., Zhou, X., Li, Y., Sun, Z., 2015. Silica nanoparticles induce oxidative stress, inflammation, and endothelial dysfunction in vitro via activation of the MAPK/Nrf2 pathway and nuclear factor-κB signaling. Int. J. Nanomed. 10, 1463–1477.

Guo, C., Yang, M., Jing, l., Wang, J., Yu, Y., Li, Y., Duan, J., Zhou, X., Li, Y., Sun, Z., 2016. Amorphous silica nanoparticles trigger vascular endothelial cell injury through apoptosis and autophagy via reactive oxygen species-mediated MAPK/Bcl-2 and PI3 K/Akt/mTOR signaling. Int. J. Nanomed. 11, 5257–5276.

Honnons, S., Porcher, J.M., 2000. In vivo experimental model for silicosis. J. Environ. Pathol. Toxicol Oncol. 19 (4), 391–400.

Kao, Y.-Y., Cheng, T.-J., Yang, D.-M., Liu -Sh, P., 2012. Demonstration of an olfactory bulb–brain translocation pathway for ZnO nanoparticles in rodent ells in vitro and in vivo. J. Mol. Neurosci. 48 (2), 464–471.

Katsnelson, B.A., Privalova, L.I., Kislitsina, N.S., Podgaiko, G.A., 1984. Correlation between cytotoxicity and fibrogenicity of silicosis-inducing dusts. Medic Lavoro 75 (6), 450–462.

Katsnelson, B.A., Privalova, L.I., Yelnichnykh, L.N., 1987. Some peculiarities of the pulmonary phagocytotic response: dust kinetics and silicosis development during long-term exposure of rats to high quartz dust levels. Br. J. Ind. Med. 44 (4), 228–235.

Katsnelson, B.A., Konysheva, L.R., Sharapova, N.Ye., Privalova, L.I., 1994. Prediction of the comparative intensity of pneumoconiotic changes caused by chronic inhalation exposure to dusts of different cytotoxicity by means of a mathematical model. Occup. Environ. Med. 51 (3), 173–180.

Katsnelson, B.A., Alekseyeva, O.G., Privalova, L.I., Polzik, E.V., 1995. Pneumoconioses: Pathogenesis and Biological Prophylaxis. The Urals Branch of the RAN, Ekaterinburg (In Russian).

Katsnelson, B.A., Makeyev, O.H., Kochneva, N.I., Privalova, L.I., Degtyareva, T.D., Bukhantsev, V.A., Minin, V.V., Beresneva, O.Y., Slyshkina, T.V., Kostyukova, S.V., 2007. Testing a set of bioprotectors against the genotoxic effect of a combination of ecotoxicants. Cent. Eur. J. Occup. Environ. Med. 13, 251–264.

Katsnelson, B.A., Degtyareva, T.D., Minigalieva, I.I., Privalova, L.I., Kuzmin, S.V., Yeremenko, O.S., Kireyeva, E.P., Sutunkova, M.P., Valamina, I.I., Khodos, M.Y., Kozitsina, A.N., Shur, V.Y., Vazhenin, V.A., Potapov, A.P., Morozova, M.V., 2011. Sub-chronic systemic toxicity and bio-accumulation of Fe_3O_4 nano- and microparticles following repeated intraperitoneal administration to rats. Int. J. Toxicol. 30 (1), 60–67.

Katsnelson, B.A., Privalova, L.I., Kuzmin, S.V., Gurvich, V.B., Sutunkova, M.P., Kireyeva, E.P., Minigalieva, I.A., 2012a. An approach to tentative reference levels setting for nanoparticles in the workroom air based on comparing their toxicity with that of their micrometric counterparts: a case study of iron oxide Fe_3O_4. ISRN Nanotechnol. 2012, 1–12. http://dx.doi.org/10.5402/2012/143613.

Katsnelson, B.A., Privalova, L.I., Sutunkova, M.P., Khodos M.Ya. Shur V.Ya. Shishkina, E.V., Tulakina, L.G., Pichugova, S.V., Beikin, J.B., 2012b. Uptake of some metallic nanoparticles by, and their impact on pulmonary macrophages in vivo as viewed by optical atomic force, and transmission electron microscopy. J. Nanomed. Nanotechnol. 3, 1–8.

Katsnelson, B.A., Privalova, L.I., Gurvich, V.B., Makeyev, O.H., Shur V.Ya. Beikin, Y.B., Sutunkova, M.P., Kireyeva, E.P., Minigalieva, I.A., Loginova, N.V., Vasilyeva, M.S., Korotkov, A.V., Shuman, E.A., Vlasova, L.A., Shishkina, E.V., Tyurnina, A.E., Kozin, R.V., Valamina, I.E., Pichugova, S.V., Tulakina, L.G., 2013. Comparative in vivo assessment of some adverse bio-effects of equidimensional gold and silver nanoparticles and the attenuation of nanosilver's effects with a complex of innocuous bioprotectors. Int. J. Mol. Sci. 14 (2), 2449–2483.

Katsnelson, B.A., Minigalieva, I.A., Privalova, L.I., Sutunkova, M.P., Gurvich, V.B., Shur, V.Ya., Shishkina, E.V., Varaksin, A.N., Panov, V.G., 2014. Lower airways response in rats to a single or combined intratracheal instillation of manganese and nickel nanoparticles and its attenuation with a bioprotective pre-treatment. Toksicol. Vestnik. 6, 8–14 (In Russian).

Katsnelson, B.A., Privalova, L.I., Sutunkova, M.P., Gurvich, V.B., Loginova, N.V., Minigalieva, I.A., et al., 2015. Some inferences from in vivo experiments with metal and metal oxide nanoparticles: the pulmonary phagocytosis response subchronic systemic toxicity and genotoxicity, regulatory proposals, searchin for bioprotectors (a self-overview). Int. J. Nanomed. 10, 3013–3029.

Kim, Y.J., Yu, M., Park, H.O., Yang, S.I., 2010. Comparative study of cytotoxicity, oxidative stress and genotoxicity induced by silica nanomaterials in human neuronal cell line. Mol. Cell. Toxicol. 6 (4), 336–343.

Kulikov, V.G., 1995. Labour Hygiene Problems and Morbidity Prevention in Workers of the Crystal Silicon Production. (Candidate of Sciences Dissertation's Published Summary). the Ural State Medical Academy, Ekaterinburg 24 pp. (in Russian).

Minigalieva, I.A., Katsnelson, B.A., Privalova, L.I., Sutunkova, M.P., Gurvich, V.B., Shur, V.Y., Shishkina, E.V., Valamina, I.E., Makeyev, O.H., Panov, V.G., Varaksin, A.N., Grigoryeva, E.V., Meshtcheryakova, E.Y., 2015. Attenuation of combined nickel (II) oxide and manganese (II, III) oxide nanoparticles' adverse effects with a complex of bioprotectors. Int. J. Mol. Sci. 16 (9), 22555–22583.

Minigaliyeva, I.A., Katsnelson, B.A., Panov, V.G., Privalova, L.I., Varaksin, A.N., Gurvich, V.B., Sutunkova, M.P., Shur, V.Ya., Shishkina, E.V., Valamina, I.E., Zubarev, I.V., Makeyev, O.H., Grigoryeva, E.V., Klinova, S.V., 2017. In vivo toxicity of copper oxide, lead oxide and zinc oxide nanoparticles acting in different combinations and its attenuation with a complex of innocuous bio-protectors (380) 72–93.

Oberdörster, G., Sharp, Z., Atudore, V., Elder, A., Gelein, R., Kreylin, W., 2004. Translocation of inhaled ultrafine particle to the brain. Inhal. Toxicol. 16 (6/7), 437–445.

Park, E.J., Park, K., 2009. Oxidative stress and pro-inflammatory responses induced by silica nanoparticles in vivo and in vitro. Toxicol. Lett. 184 (1), 18–25.

Petin, L.M., 1978. Data for establishing the maximal allowable concentration of silica-containing condensation aerosols. Gigiyena Truda 6, 28–33 (In Russian).

Petrick, L., Rosenblat, M., Paland, N., Aviram, M., 2016. Silicon dioxide nanoparticles increase macrophage atherogenicity: stimulation of cellular cytotoxicity, oxidative stress, and triglycerides accumulation. Environ. Toxicol. 31 (6), 713–723.

Privalova, L.I., Katsnelson, B.A., Osipenko, A.B., Yushkov, B.H., Babushkina, L.G., 1980. Response of a phagocyte cell system to products of macrophage breakdown as a probable mechanism of alveolar phagocytosis adaptation to deposition of particles of different cytotoxicity. Environ. Health Perspect. 35, 205–218.

Privalova, L.I., Katsnelson, B.A., Loginova, N.V., Gurvich, V.B., Shur, V.Y., Valamina, I.E., Makeyev, O.H., Sutunkova, M.P., Minigalieva, I.A., Kireyeva, E.P., Rusakov, V.O., Tyurnina, A.E., Kozin, R.V., Meshtcheryakova, E.Y., Korotkov, A.V., Shuman, E.A., Zvereva, A.E., Kostykova, S.V., 2014a. Subchronic toxicity of copper oxide nanoparticles and its attenuation with the help of a combination of bioprotectors. Int. J. Mol Sci. 15 (7), 12379–12406.

Privalova, L.I., Katsnelson, B.A., Loginova, N.V., Gurvich, V.B., Shur, V.Y., Beikin, Y.B., Sutunkova, M.P., Minigalieva, I.A., Shishkina, E.V., Pichugova, S.V., Tulakina, L.G., Beljayeva, S.V., 2014b. Some characteristics of free cell population in the airways of Rrats after intratracheal instillation of copper-containing nano-scale particles. Int. J. Mol. Sci. 15 (11), 21538–21553.

Robock, K., 1973. Standard quartz DQ 12 < 5 mcm for experimental pneumoconiosis research project in the Federal Republic of Germany. Ann. Occup. Hyg. 16, 63–66.

Rylova, M.L., 1964. Methods of Investigating Long-term Effects of Noxious Environmental Agents in Animal Experiments. Meditsina, Leningrad (in Russian).

Sergent, J.A., Paget, V., Chevillard, S., 2012. Toxicity and genotoxicity of nano-SiO_2 on human epithelial intestinal HT-29 cell line. Ann. Occup. Hyg. 56 (5), 622–630.

Sutunkova, M.P., Katsnelson, B.A., Privalova, L.I., Gurvich, V.B., Konysheva, L.K., Shur, V.Ya., Shishkina, E.V., Minigalieva, I.A., Solovjeva, S.N., Grebenkina, S.V., Zubarev, I.V., 2016. On the contribution of the phagocytosis and the solubilization to the iron oxide nanoparticles retention in and elimination from lungs under long-term inhalation exposure. Toxicology 363, 19–28.

Tietz, N.W., 1995. Clinical Guide to Laboratory Tests, 3rd ed. W.B. Saunders Company, Philadelphia, PA, USA 942 pp.

Vance, M.E., Kuiken, T., Vejerano, E.P., McGinnis, S.P., Hochella, M.F.Jr., Rejeski, D., Hull, M.S., 2015. Nanotechnology in the real world: redeveloping the nanomaterial consumer products inventory. Beilstein J. Nanotechnol. 6, 1769–1780.

Velichkovsky, B.T., Katsnelson, B.A., 1964. Aetiology and Pathogenesis of Silicosis. Meditsina Publishers, Moscow (In Russian).

Wang, J., Yu, Y., Lu, K., Yang, M., Li, Y., Zhou, X., Sun, Z., 2017. Silica nanoparticles induce autophagy dysfunction via lysosomal impairment and inhibition of autophagosome degradation in hepatocytes. Int. J. Nanomed. 12, 809–825.